Journal of Anatomy

J. Anat. (2017) doi: 10.1111/joa.12601

A detailed musculoskeletal study of a fetus with anencephaly and spina bifida (craniorachischisis), and comparison with other cases of human congenital malformations

Malak A. Alghamdi,[1] Janine M. Ziermann,[1] Lydia Gregg[2] and Rui Diogo[1]

[1]*Department of Anatomy, Howard University College of Medicine, Washington, DC, USA*
[2]*Division of Interventional Neuroradiology, Department of Art as Applied to Medicine, Johns Hopkins University School of Medicine, Baltimore, MD, USA*

Abstract

Few descriptions of the musculoskeletal system of humans with anencephaly or spina bifida exist in the literature. Even less is published about individuals in which both phenomena occur together, i.e. about craniorachischisis. Here we provide a detailed report on the musculoskeletal structures of a fetus with craniorachischisis, as well as comparisons with the few descriptions for anencephaly and with musculoskeletal anomalies found in other congenital malformations. We focused in particular on the comparison with trisomies 13, 18, and 21 because neural tube defects have been associated with such chromosomal defects. Our results showed that many of the defects found in the fetus with craniorachischisis are similar not only to anomalies previously described in the available works on musculoskeletal phenotypes seen in fetuses with anencephaly and spina bifida, but also to a wide range of other different conditions/syndromes including trisomies 13, 18 and 21, and cyclopia. The fact that similar anomalies are seen commonly not only in a wide range of different syndromes, but also as variants of the normal human population and as the 'normal' phenotype of other animals, supports Pere Alberch's unfortunately named idea of a 'logic of monsters'. That is, it supports the idea that development is so constrained that both in 'normal' and abnormal development one sees certain outcomes being produced again and again because ontogenetic constraints only allow a few possible outcomes, thus also leading to cases where the anatomical defects of some organisms are similar to the 'normal' phenotype of other organisms. In fact, this applies not only to specific anomalies but also to general patterns, such as the fact that in pathological conditions affecting different regions of the body, one consistently sees more defects on the upper limbs than on the lower limbs. Such general patterns are, again, seen in the fetus examined for this study, which had 29 muscle anomalies on the right upper limb and 22 muscle anomalies on the left upper limb, vs. seven muscle anomalies on the right lower limb and two on the left lower limb. It is therefore hoped that this work, which is part of our effort to describe and compile information on human musculoskeletal defects found in a wide range of conditions, will contribute not only to a better understanding of craniorachischisis in particular and of human congenital malformations in general, but also to broader discussions on the fields of comparative anatomy, and developmental and evolutionary biology.

Key words: anencephaly; birth defects; bones; comparative anatomy; craniorachischisis; fetus; human anatomy; muscles.

Introduction

Craniorachischisis is a condition marked by a neural tube defect that results in the absence of the majority of the skull and brain (anencephaly) combined with an open vertebral column (spina bifida). It is also defined as a caudal extension of anencephaly (Wyszynski, 2006), with the most

Correspondence
Rui Diogo, Department of Anatomy, Howard University College of Medicine, Numa Adams Building, Room 1101, 520 W St. NW, Washington DC, 20059, USA. T: + 1 202 6400982; F: + 1 202 5367839; E: rui.diogo@howard.edu

Accepted for publication *16 January 2017*

severe condition called craniorachischisis totalis in which the entire length of the neural tube opens onto the surface of the head and back (Oostra et al. 1998; Schoenwolf et al. 2015). In particular, anencephaly results from failure of the cranial portion of the neural tube to fuse, whereas spina bifida results from failure of the caudal portion to fuse. In addition, anencephaly is a partial or complete absence of cranial vault (frontal, parietal, occipital, temporal, sphenoid and ethmoid bones) with absence of overlying tissues and malformation and damage of fundamental brain structures (Lazareff, 2011). Anencephaly is one of three neural tube defects that affect the cranial bones; the other two are encephalocele and iniencephaly (Lazareff, 2011).

Craniorachischisis is a rare and severe form of neural tube defects (NTDs; Wyszynski, 2006; Coskun et al. 2009). It appears in the cervico-thoracic region, where normally a distinct median hinge point (MHP, Fig. 1) should form without clear morphological evidence of dorsolateral hinge points (DLHP, Fig. 1), resulting in an ovoid neural tube and slit-shaped central canal. Defects in normal development by interference of MHP formation will lead to normal but widely spaced neural folds that prevent proper fusion (Detrait et al. 2005). Features commonly present in fetuses with craniorachischisis are protruding eyes, cleft palate and/or lip, and short or absent neck (Vare & Bansal, 1971). The protruded/bulging eyes give the craniorachischisis fetus a typical ultrasound appearance of 'frog's eyes' and may be due to the receded superciliary ridges caused by failure of forehead formation (Nañagas, 1925), or by a shortening of the anterior cranial fossa (Sucheston & Cannon, 1970). In order to provide a basis for understanding the mechanisms that are affected by craniorachischisis and the anatomies associated with this condition, we thus need to present an introduction to normal neural tube formation, and then of neural tube defects commonly seen in humans.

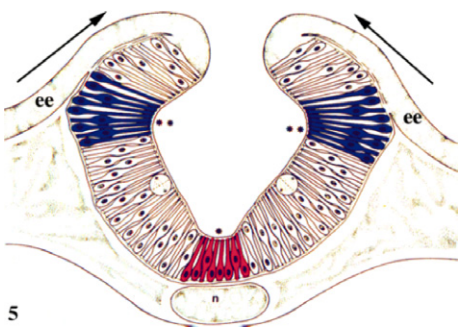

Fig. 1 Illustration of the hinge points model of bending of the chick neural plate. Neuroepithelial cell wedging within the hinge points is indicated by red (median hinge point) and blue (dorsolateral hinge points). Arrows indicate mediolateral expansion of the epidermal ectoderm; single asterisk indicates furrowing associated with the median hinge point. Double asterisks indicate furrowing associated with the dorsolateral hinge points. ee, epidermal ectoderm; n, notochord (modified from Colas & Schoenwolf, 2001).

Regarding *normal neural tube formation*, the neural tube is the embryonic structure that develops into the central nervous system (CNS) (Detrait et al. 2005; Klein, 2013). The process of neural tube formation, or neurulation, occurs between weeks 3 and 4 of the embryonic development (Detrait et al. 2005; Lazareff, 2011; Schoenwolf et al. 2015). Neurulation involves four main events: formation of the neural plate, folding, convergence, and fusion. The first event in the development of the future CNS is caused by neural induction that leads to a thickening of the ectoderm above the notochord, which forms due to migrating epiblast cells (outer or ectodermal layer of the two-layered embryo) through the primitive node anteriorly. The resulting ectodermal thickening is called the neural plate and is located cranial to the primitive node (Lazareff, 2011; Schoenwolf et al. 2015). The neural plate extends and, by the end of week 3, consists of a broad portion cranially and a narrow portion caudally that give rise to the brain and spinal cord, respectively (Schoenwolf et al. 2015).

The second event, folding, is characterized by the lateral neural fold development that is caused by cells along the MHP undergoing apical constriction, which leads to the appearance of the neural groove between the neural folds. The neural folds elevate dorsally by rotating around the central pivot point of the MHP (Fig. 1), to form the neural groove. The third event, convergence, is the apical constriction of two DLHPs, which leads to the development of a tube-like structure (i.e. lateral folds moving towards each other and deepening of the neural groove to form the neural tube). The fourth and final step of neurulation is the fusion of the dorsal-most cells on each cell of the neural tube and the fusion of the epidermis dorsal to the neural tube. It involves adhesion of the neural folds to one another and subsequent rearrangement of cells within the folds to form two separate epithelial layers (Schoenwolf et al. 2015). According to some authors, the closing of the neural groove starts at a single site and extends bi-directionally, rostrally and caudally, in a zipper-like process (Keiller, 1922; Detrait et al. 2005; Schoenwolf et al. 2015). In contrast, other authors identify various separate sites for neural tube closure (Van Allen et al. 1993; Golden & Chernoff, 1995; Lazareff, 2011). According to Golden & Chernoff (1995), four sites of closure in the anterior neural tube have been defined so far: closure I starts in the cervical region and extends bilaterally; closure II begins at the prosencephalic-mesencephalic (forebrain-midbrain) border and extends bilaterally; closure III is initiated adjacent to the stomodeum (precursor of the mouth and the anterior lobe of the pituitary gland) and extends caudally to meet closure II; closure IV takes place above the rhombencephalon (hindbrain) and extends to meet closure II (Fig. 2).

Neural tube defects (NTDs) are congenital malformations of the CNS that are caused by partial or complete failure of the neural tube to close in the third and fourth weeks of pregnancy (within 28 days after conception; Klein, 2013).

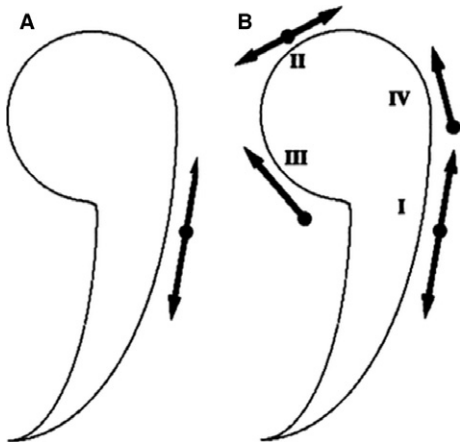

Fig. 2 Diagram showing the two models of anterior neural tube closure: (A) the 'zipper' or continuous closure, (B) and the multi-sites closure pattern. Closure I starts in the cervical region and extends bilaterally; closure II begins at the prosencephalic-mesencephalic (forebrain-midbrain) border and extends bilaterally; closure III is initiated adjacent to the stomodeum (precursor of the mouth and the anterior lobe of the pituitary gland) and extends caudally to meet closure II; and closure IV takes place above the rhombencephalon (hindbrain) and extends to meet closure II. (Modified from Golden & Chernoff, 1995).

This failure occurs when neurulation is disrupted or misregulated, and the neural tube can thus be open to the surface, which is the most severe type of defect (Schoenwolf et al. 2015). Specifically, the anatomical classification of NTDs is: (i) cranial defects including anencephaly; and (ii) spinal defects including spina bifida. Both types can involve closed or open neural tubes (Lazareff, 2011). NTDs are listed as 'rare diseases' by the Office of Rare Diseases of the National Institutes of Health (NIH; Klein, 2013), being the second most common type of birth defects (after congenital heart defects), with a birth incidence of about 1/1000 in American Caucasians (Detrait et al. 2005).

Anencephaly and myelomeningocele (spina bifida with protruding spinal cord; most severe form of spina bifida) are the most severe forms of NTDs and result from failure of the neural tube to fully close in the developing brain or in the lower spine, respectively. Craniorachischisis is considered to be a rare disorder in most populations (Klein, 2013). Infants with anencephaly usually die shortly after birth, whereas children born with spina bifida tend to survive but might have disabilities and the need of chronic health care, dependent on the type of spina bifida. Therefore, many women choose to terminate their pregnancy when a severe NTD is detected prenatally (Klein, 2013).

In humans, NTDs are multifactorial disorders, resulting from both genetic and epigenetic factors (Detrait et al. 2005; Klein, 2013). More than 80 mutations in different genes have been identified and linked to a variety of rodent NTDs, for instance. However, the mechanisms by which NTDs arise are generally unclear, even when the mutated gene has been identified (Detrait et al. 2005). Carlson (1981) noted that the inductive influence provided by the developing brain is necessary for initiation of ossification of the dermal skull roof, which might explain why fetuses with anencephaly seem to lack the bones that normally form the roof of the skull.

Epigenetic factors related to NTDs include several maternal conditions and/or habits, such as diabetes, obesity, use of anti-convulsant medications (treatment of epilepsy), and exposure to solvents through house cleaning (Detrait et al. 2005). Several studies have shown that maternal peri-conceptional supplement with folic acid lowers the occurrence risk for NTDs; the folic acid supplementation can prevent up to two-thirds (70%) of NTD pregnancies. Approximately, 15–25% of human infants with NTDs have associated defects. The most common ones, found with a frequency of 1–6%, are facial clefts, small or absent ears and eyes, limb deficiencies, cardiac defects, abdominal wall defects, and renal anomalies (Moore et al. 2011).

There are almost no descriptions in the literature of the musculoskeletal system of humans with anencephaly, with spina bifida, and with both conditions together, i.e. with craniorachischisis. It is therefore hoped that the musculoskeletal descriptions that will be provided here, as well as the comparisons with the very few descriptions available in the literature for these conditions, and with musculoskeletal anomalies found in other congenital malformations, will contribute to a better understanding of craniorachischisis in particular, and of human congenital malformations in general. Our comparison focuses in particular on trisomies 13, 18, and 21 because NTDs have been associated with such chromosomal defects (Wyszynski, 2006; Lazareff, 2011). Importantly, this work is part of our effort to describe and compile information on human musculoskeletal defects found in a wide range of conditions, including for instance trisomy and cyclopia (e.g., Diogo et al. 2015; Smith et al. 2015).

Materials and methods

A male fetus with craniorachischisis (anencephaly with spina bifida) was dissected at Rui Diogo's lab, Department of Anatomy, Howard University College of Medicine. The fetus is part of a collection obtained in the 1980s by Prof. Aziz, which was donated to Diogo's lab for research. The age was estimated to be 7 months of gestation and is the result of the comparison of the external characteristics of the fetus with those of normal fetuses (England, 1983), but taking into account that individuals with congenital malformations often have a developmental delay in specific characteristics. Therefore, the fetus was also compared with the literature and our own work (Diogo et al. 2015; Smith et al. 2015). In addition to external comparison, we described various musculoskeletal structures, and also included CT scans for the analysis of skeletal structures. These scans show all calcified bones, and were thus crucial to the preparation of the muscle dissections and subsequently dissection of all skeletal structures in detail. Specifically, the CT datasets were generated from a 20-s rotational flat panel CT acquisition, an imaging

technique that produces volumetric datasets with a high spatial resolution using a C-arm X-ray system, and reconstructed on a dedicated workstation (0.1–0.4 mm voxel size).

Dissections were performed using standard microdissection tools. Muscles were the special focus of the microdissections; nerves and major blood vessels were preserved wherever possible. Superficial muscles were cut close to their attachment and reflected to observe the deeper muscles. Complete detachment was avoided to preserve the integrity of the muscles if needed for further studies. The following characters of each muscle were observed: (i) presence/absence, (ii) origin, (iii) insertion, (iv) variation in number of bellies and/or tendons, and (v) overall muscular configuration. Muscles were compared with those of 'normal' human adults as well as 'normal' fetuses, based on our previous dissections of fetuses (e.g. Diogo et al. 2015; Smith et al. 2015) and on descriptions previously published by others (e.g. Bardeen & Lewis, 1901; Lewis, 1902, 1910; Netter, 2012). Photos were taken as a reference using a Nikon D90 camera with an AF-S Micro NIKON 60-mm lens at each stage of the dissection to document different anatomical regions. Pins were placed under or next to the bellies of the muscles to emphasize a specific muscle. A standard centimeter scale was placed into each photograph for size reference. The hand and foot muscles were micro-dissected under a dissection microscope (Nikon AZ100) and photographed with an attached camera (Nikon DS-Fi1; software NIS-Elements D4.00.03).

Results

External features of the fetus

The CNS of the fetus was severely affected. The open cranium did not contain a brain but some neural tissue seemed to be present; the vertebral column was open with no posterior vertebral arches and spinal cord. Gray tissues occupied the opened cranium (meninges). Long, dark hair surrounded the superior and right sides of the neural tissue. Skin covered the whole body except the open cranium and vertebral column (Fig. 3). The eyes were large and protruded, and the eyelashes were developed. A right cleft palate with cleft lip was observed, and the tongue was protruded. The head was tilting to the right side, consequently the right eye was located immediately superior to the right shoulder, and the right ear was anterior to it. The neck was atrophied, and the ears were displayed inferiorly (Fig. 4).

Fig. 3 Posterior view of the fetus with craniorachischisis, showing the NTD with open cranium and spinal cord (right figure), and CT scan of the skeletal system (left figure). Scale bar: 1 cm.

The right upper limb was more affected than the left one. It was shorter; four digits were present on the right hand; and the long axis of the hand was perpendicular to the long axis of the arm. In addition, both hands were enlarged, relative to the body size, compared with those in normal fetuses of the same age; the fingernails reached the tip of the fingers. The morphology of the right lower limb was similar to that of the left lower limb. The fetus had rocker bottom feet (Fig. 3), which were larger than in normal fetuses when compared with the body size. The toenails did not reach the tip of the toes, and the skin that covered the heels of the feet was extremely wrinkled. The left ankle was severely dorsiflexed with the dorsum of the foot touching the anterior side of the leg. The abdominal wall of the fetus was open, and the intestines protruded outside the abdomen in a sac (a condition designated as omphalocele: Fig. 4).

Skeleton

The fetal skeleton was studied with CTs. The *parietal* and the *squamous part of the temporal* bone seemed to be absent (Figs 5 and 6). The *frontal* bone was narrow and separated in the middle line, and it formed the superior margin of the orbits. The occipital bone develops from seven embryonal structures, all of which could be identified in the specimen studied. The *single basioccipital* was located posterior to the sella turcica of the sphenoid bone; a pair of *exooccipital* bones was positioned infero-lateral to the basioccipital; a pair of flat *supraoccipital* bones lay lateral to the two exooccipital bones; and a pair of *interparietal* bones were fused to the anterior border of the exooccipital bones, the left interparietal being long and attached to the lateral corner of the left frontal bone, while the right interparietal was not (Figs 5 and 6).

Two thin *zygomatic* bones formed the lateral margin of the orbits; each bone had a small *temporal process*. A pair of *maxillary* bones formed the infero-medial margin of the orbits; they were separated by fused *nasal* bones. The lower *mandible* consisted of two separated asymmetrical bones: the left had a body and a ramus, and it articulated with the *petrous part* of the temporal bone; the right had a body without ramus, and its lateral-inferior border was next and perpendicular to the right *clavicle* (Figs 6 and 7). No complete *hyoid* complex could be observed, with just a few parts of it being seemingly present. Instead, a *hyoid arcade*, i.e. an arch made of strong fascia that resembles the arcade found in many non-human primates but that is usually not present in humans (Diogo & Wood, 2011, 2012), was

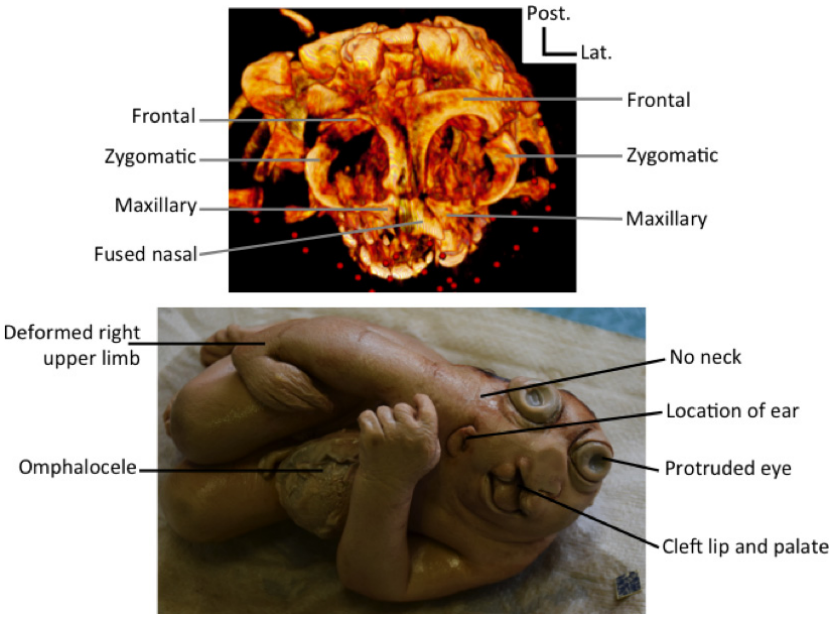

Fig. 4 Anomalies of the craniorachischisis fetus in anterior view. Upper figure: CT scan of the head showing the facial bones and the associated deformities. Lower figure: *in situ* view of the specimen with obvious malformations indicated. Scale bar in the lower figure: 1 cm.

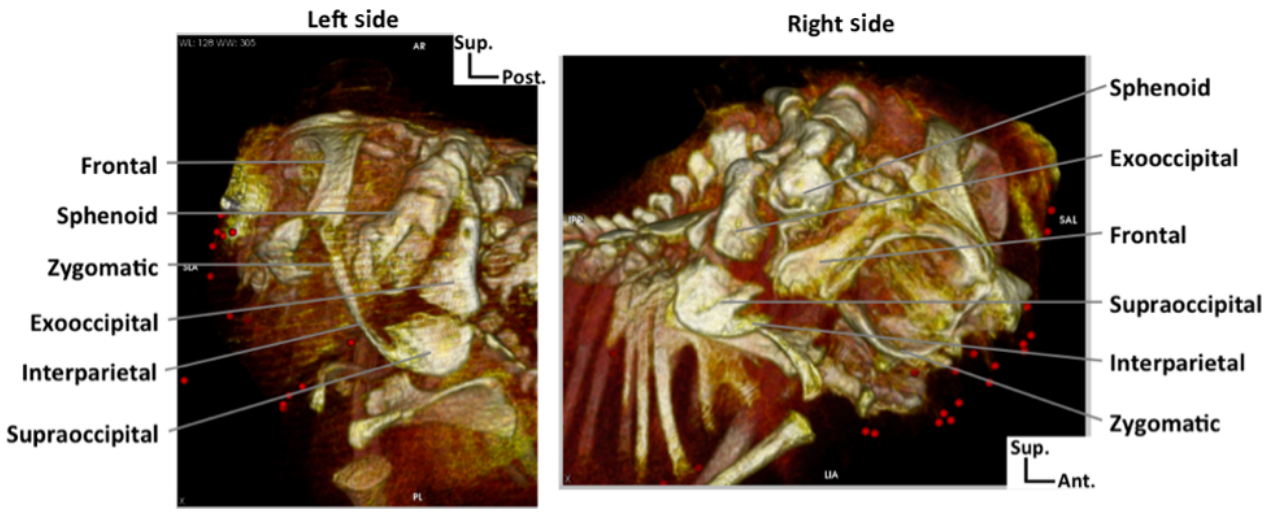

Fig. 5 CT scans of the fetus with craniorachischisis, showing the bones of the cranial vault. In this and all subsequent figures, as well as in Fig. 4: Ant, anterior; Inf, inferior; Lat, lateral; Med, medial; Post, posterior; Sup, superior. Scale bar: 1 cm.

present in the hyoid region, and muscles were attached to it, including hypobranchial infrahyoid muscles (Figs 7 and 13). There was no styloid process on the right side, and that of the left side was thicker than normal. The stylohyoid ligament was observed on the left side, running from the styloid process to the hyoid arcade. The thyroid, arytenoid and cricoid cartilages appeared normal.

Observed characters on the postcranial skeleton: 11 *ribs* were counted on the left side and fused ribs were seen on the right side; 19 *vertebral* bodies (3 cervical, 8–10 thoracic, 4 lumbar, sacrum, paired coccyx; Fig. 3) that had different sizes were counted (the thoracic discrepancy of the count depends on how one evaluates the vertebral fragments in the mid-thoracic region); the right and left *clavicles* were located immediately inferior to the mandible. The left *scapula* seemed to be normal whereas the right scapula was reduced in size. The left upper limb had a normal *humerus*, *radius* and *ulna*, five incompletely ossified *metacarpals*, and 14 *phalanges*, i.e. all normal phalanges were present. The right upper limb had a broken humerus, no radius, bowed (curved) ulna, only four metacarpals (metacarpal 1 missing, and metacarpal 2 is reduced), and 10 phalanges. That is, digit 1, i.e. the thumb, was completely missing and in addition the proximal and distal phalanges of digit 2, which is vestigial, were also missing (Fig. 8): reduction, or even complete absence of the index finger, have been described in

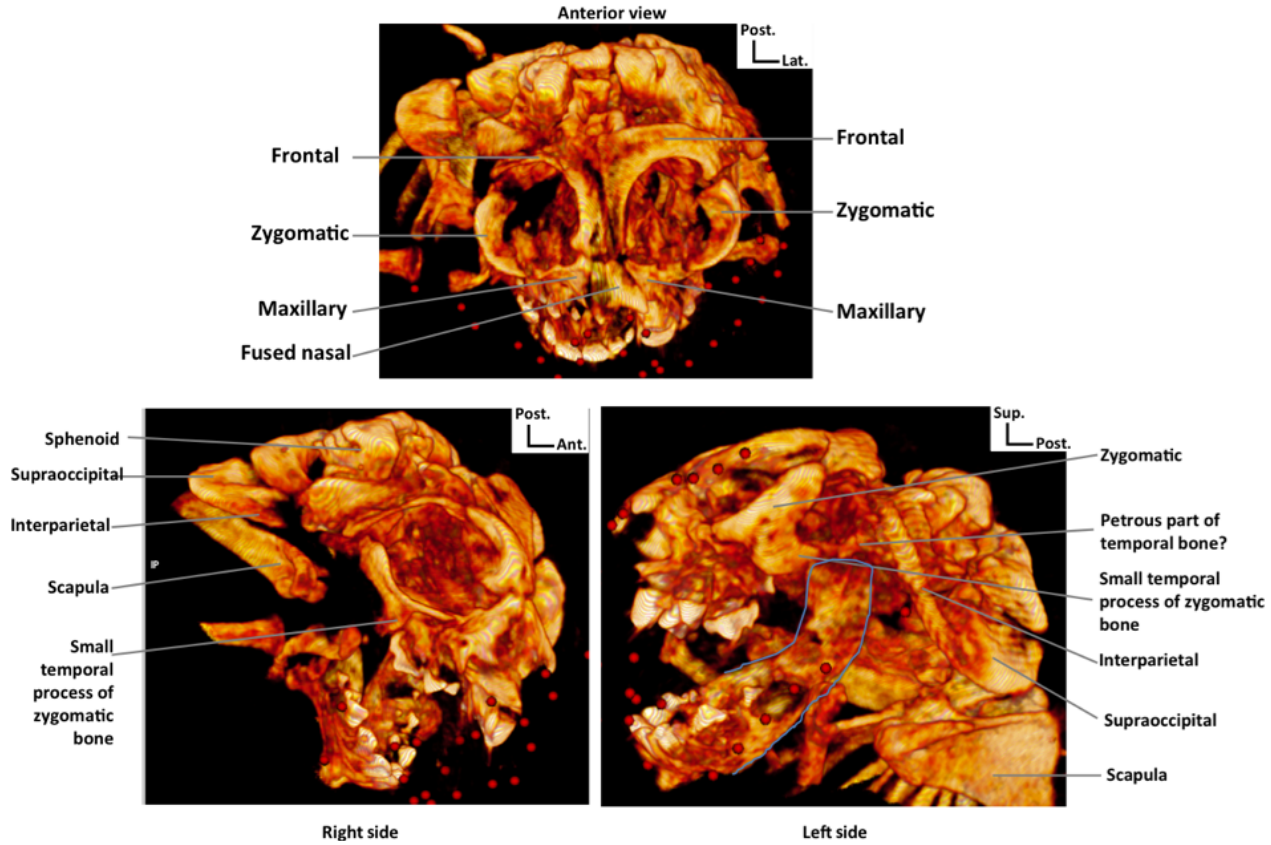

Fig. 6 CT scans of anterior (upper figure) and lateral views (lower figures) of the fetus with craniorachischisis, showing the facial bones.

congenital malformations involving radial deficiency (e.g. Rayan & Upton, 2014). Dissection of the hand showed that the carpal cartilages were normal in number and location on the left hand only. On the right hand, the *pisiform* and *hamate* were the only separated cartilages; the other carpal cartilages were fused together to form a single structure articulating with each of the remaining digits, i.e. digit 4, digit 3, and the vestigial digit 2.

The hip had three separated bones in each side: *ilium*, *ischium*, and *pubis*, which had no apparent malformation. The lower limb bones also seemed to be completely normal: the *femur*, *tibia*, *fibula*, *calcaneus*, *talus*, five *metatarsals*, and 14 *phalanges* were observed.

Muscles

We focus here on the description of anomalies. Those and the normal attachments with remarks on the malformation are detailed in Supporting Information Tables S1–S6. Notes on identified nerves are made in the tables and are only described in the text if they were unusual.

Muscles of the right upper limb (Table S1)

The right *latissimus dorsi* was clearly smaller than the left one and originated from the unfused (open) thoracic and lumbar vertebrae and the iliac crest. The *levator scapulae* was missing. The *deltoideus* had a normal configuration but seemed to be fused with the *pectoralis major* muscle. No deltopectoral triangle was observed, but such a fusion is not uncommon for humans. The pectoralis major originated from the sternum and the clavicle, the muscle fibers extended laterally and inferiorly, the muscle then was split into two bands, one inserted onto the crest of the greater tubercle of the humerus and the other extended inferiorly and attaching to the medial supracondylar ridge of the humerus. This latter bundle has some similarities with the abnormal muscle 'costohumeralis' sometimes seen in humans (e.g. Rao et al. 2009). Upon reflecting the pectoralis major, the *dorsoepitrochlearis* muscle was visible and fused distally to the inner side of the inferior ('costohumeralis') band of the pectoralis major (Fig. 9). This muscle is normally not seen in humans but is found in most other primates, where it originates proximally from the latissimus dorsi (Diogo & Wood, 2011, 2012).

The posterior shoulder muscles, *supraspinatus, infraspinatus*, and *teres major* and *minor,* had mainly normal proximal and distal attachments. As found in many 'normal' humans, there was a fusion between the proximal halves of the infraspinatus and teres minor. Abnormally, the *pectoralis minor*, the short head of *biceps brachii*, and the *coracobrachialis* attached to the lesser tubercle of the humerus

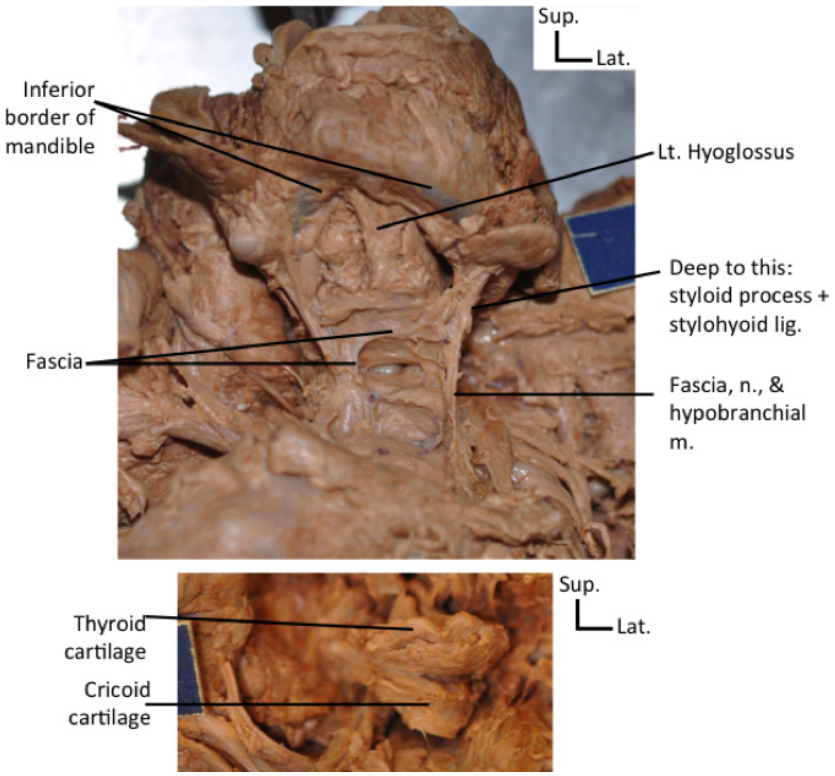

Fig. 7 Anterior views of the neck of the fetus with craniorachischisis, showing absence of hyoid bone and presence of a hyoid arcade instead, which is somewhat similar to that often present in non-human mammals (upper figure), and thyroid and cricoid cartilages that are apparently normal (lower figure). The hyoid arcade was connected to hypobranchial muscles, which are shown in more detail in Fig. 13. Lig, ligament; Lt, left; m, muscles; n, nerve. Scale bar: 1 cm.

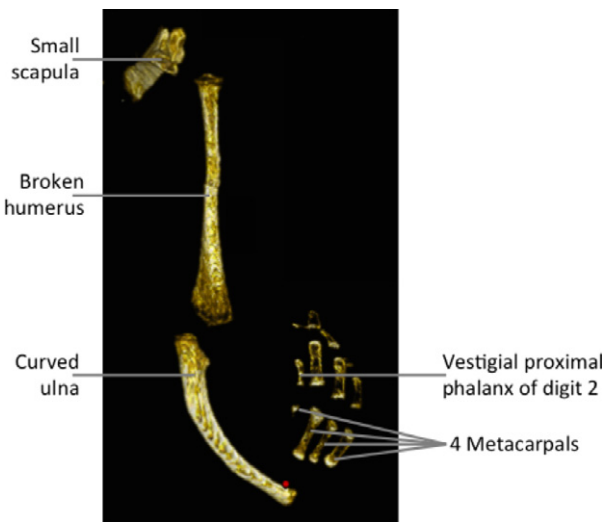

Fig. 8 CT of lateral view of the right upper limb of the fetus with craniorachischisis, showing bone malformations.

instead of the coracoid process of the scapula (Fig. 9). The lower attachment of the pectoralis minor was to ribs 2–4, and the short head of the biceps and the coracobrachialis attached to the lateral condyle and medial supracondylar ridge of the humerus, respectively, so these latter insertions were also abnormal. Furthermore, the distal end of coracobrachialis and dorsoepitrochlearis and inferior ('costohumeralis') band of the pectoralis major were fused, and the long head of biceps brachii and the *brachialis* were seemingly absent (Fig. 9). Abnormally, the *triceps brachii* had four heads. The proximal origins of the three normal – i.e. long, lateral and medial – heads and their common insertion were normal. The fourth, abnormal, head arose from the lateral side of the humerus inferior to the deltoid, with some of its fibers extending anteriorly and attaching to the anterior side of the medial condyle and the other fibers extending posteriorly to attach to the olecranon process of the ulna.

Relative to the pectoral and arm regions, more anomalies were found at the level of the forearm. The superficial layer had four muscles, from medial to lateral: *flexor carpi ulnaris*, *palmaris longus, flexor digitorum superficialis,* and *pronator teres.* The deep layer had four muscles: *flexor digitorum profundus*, and three abnormal small muscles that seem to be derived from this muscle. The flexor carpi ulnaris was a broad muscle that originated from the medial side of the medial epicondyle of the humerus, the olecranon process of the ulna, and the shaft of the ulna, and attached distally to the pisiform cartilage as usual, but without forming the usual tendon. The palmaris longus had normal attachments, but its proximal end was abnormally fused with the flexor carpi ulnaris. The flexor digitorum superficialis was reduced in size, originating from the medial epicondyle of the humerus as usual, but sending tendons to digits 3 and 4 only (not to digit 5, or to digit 2, which was vestigial), with the usual bifurcation of each tendon at the level of the attachment to the middle phalanges of digits 3 and 4. The

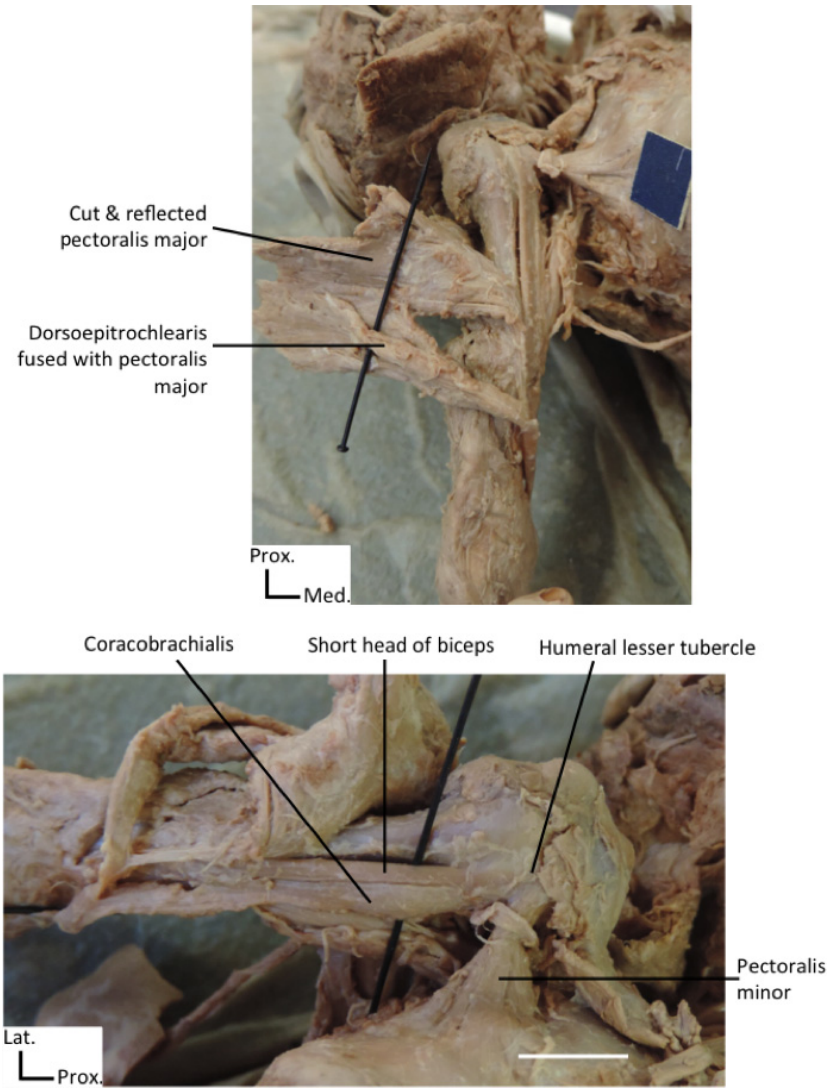

Fig. 9 Anterior views of the right arm showing a dorsoepitrochlearis muscle – a muscle normally present in non-human mammals – fused to the inner side of the pectoralis major (upper figure) and the short head of the biceps brachii, the coracobrachialis, and the pectoralis minor attached to the lesser tubercle of the humerus (lower figure). Scale bar in the upper figure: 1 cm.

pronator teres was a thin long muscle originating from the medial epicondyle of the humerus; its muscle fibers extended obliquely in a normal direction but then extended abnormally distally to attach to the fascia at the level of the hand. The *flexor carpi radialis*, *flexor pollicis longus*, and *pronator quadratus* were not observed on the right forearm.

The main body of the flexor digitorum profundus arose from the posterior side of the ulnar shaft and attached by two tendons to the distal phalanges of the two most medial digits, i.e. digits 4 and 5 (not 3; or to the vestigial digit 2). Each of the tendons to digits 4 and 5 gave rise to a *lumbrical*, and the tendon going to digit 4 passed deep to the tendon of flexor digitorum superficialis to that digit, as usual. The ulnar nerve passed between the superficial and deep layers of the forearm flexor muscles, and sent four major branches to the hypothenar muscles and the medial two and half digits, as usual. Two bundles of the flexor digitorum profundus are deeper to the main body of this muscle. One of these bundles originates from the shaft of the ulna that had two tendons: one attached to connective tissue on the anterior side of the distal end of the forearm, and the other joined the tendon from the other deep bundle, which passed deep to and joined the tendon of the flexor digitorum superficialis going to digit 3, then attaching to the distal phalanx of this digit as the tendon of the flexor digitorum profundus usually does. So, in total, the flexor digitorum profundus attached onto digits 3, 4, and 5.

The posterior forearm muscles had a particularly abnormal overall configuration (Fig. 10). The superficial layer had four muscles: *the anconeus*, and three superficial extensor muscles, which we designated '1', '2', and '3' in Fig. 10 and which seem to correspond to the *extensor digitorum*, *extensor digiti minimi*, and *extensor carpi ulnaris*, respectively. The middle layer consisted of a big sheet of muscle fibers with a central tendon attached to the extensor retinaculum at the tip of the ulna. The deepest layer included: *abductor pollicis longus*, *extensor pollicis longus*, and *extensor indicis*.

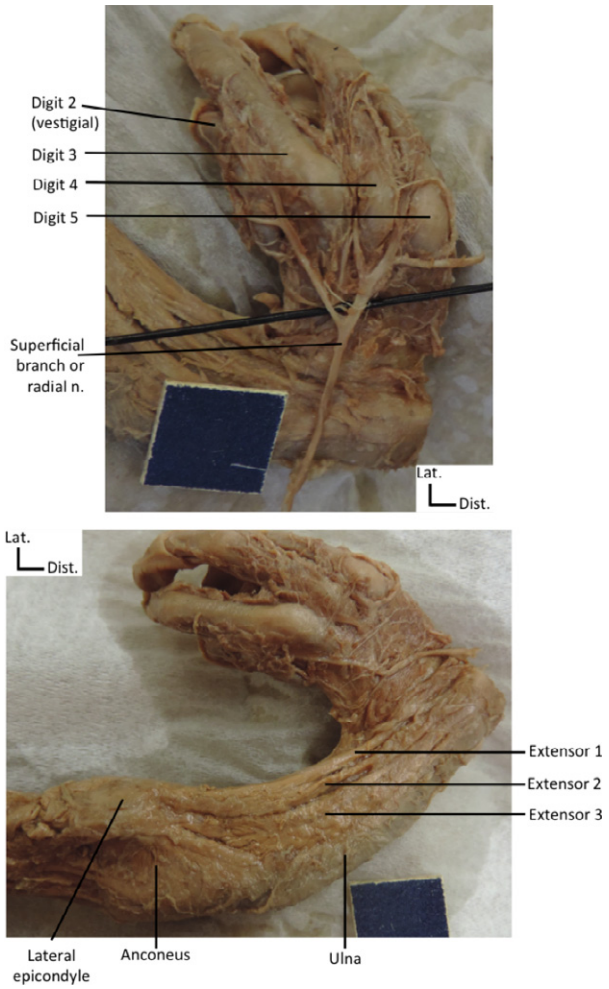

Fig. 10 Posterior view of the right forearm and hand of the fetus with craniorachischisis showing the superficial nerves and muscles and the digits. Scale bar: 1 cm.

The extensor digitorum had a normal origin, but had three insertions: an abnormal tendon to the ulnar styloid process, a normal tendon to digit 3, and a third, abnormal, tendon that split before and passed deep to the previous two tendons and then attached to digit 5. The extensor digiti minimi had a normal origin and inserted distally onto digit 5, as usual via a tendon that passed deep to the 1st tendon and medial to the 3rd tendon of the extensor digitorum. The extensor carpi ulnaris and anconeus showed no anomalies.

In the deepest layer, the muscle fibers originated from the shaft of the ulna and were arranged into three groups/muscles without definite borders: two deep transverse muscles and one superficial longitudinal muscle (Fig. 10). The superior transverse muscle fibers attached distally to a fascia/connective tissue and can be tentatively interpreted as the *extensor pollicis longus*; the inferior transverse muscle fibers sent a small tendon to digit 4 (not to digit 2 as usual, which was vestigial) and can be interpreted as the *extensor indicis*; and the superficial longitudinal muscle fibers attached to the extensor expansion and can be interpreted as an *abductor pollicis longus*.

Only 10 hand muscles were present (Fig. 11): two lumbricals originated from two tendons of the flexor digitorum profundus as described above, and inserted onto digits 4 and 5; the three usual hypothenar muscles, which will be described below; two palmar interossei (to radial sides of digits 5 and 4, respectively); and three dorsal interossei. The *abductor digiti minimi*, *opponens digiti minimi*, and *flexor digiti minimi* had normal attachments.

Muscles of the left upper limb (Table S2)

The left *latissimus dorsi* had similar attachments as the right one, but there was an anomalous muscle slip between the left latissimus dorsi and the left triceps brachii. Upon reflecting the left trapezius and pulling the head away from the shoulder, three longitudinal muscles originated from the superior angle of the scapula. The most lateral one is an anomaly: it is the *rhomboideus occipitalis*, which is normally present in non-human primates but not in humans (Diogo & Wood, 2011, 2012), extending from the scapula to the supraoccipital bone. The middle one, *levator scapulae*, was abnormally fused with the distal half of the middle scalene and was attached to the cervical vertebrae, as normal. The deeper middle muscle seemed to be part of the levator scapulae with an abnormal attachment to the occipital rhomboid, as it attached to the supraoccipital bone, or could instead be a separated part of the occipital rhomboid.

The *deltoideus* had normal attachments, and similarly to the right side there was no clear deltopectoral triangle due to fusion of the deltoid and pectoralis major. The *pectoralis major* originated from the clavicle, sternum, and costal cartilages, but only a few fibers attached to the crest of the greater tubercle, whereas most of the fibers attached to the deltoid tuberosity with the deltoid. On the inner side of the pectoralis major, a small abnormal muscle was observed originating from the anterior capsule of the shoulder joint and attaching distally to the fibers of the pectoralis major, which attached to the crest of the greater tubercle. The *pectoralis minor* arose from ribs 3–5 and attached to the coracoid process of the scapula, i.e. it had a normal insertion, contrary to that of the right side of the body, but it did have a small abnormal muscle slip connecting it to the pectoralis major.

The *supraspinatus*, *infraspinatus*, *teres minor*, and *teres major* had mainly normal attachments. The proximal third of the infraspinatus and teres minor muscles were fused, as often seen in 'normal' humans, but there was a clearly abnormal slip between the teres major and the long head of the *biceps brachii*. There was a thin layer of short muscle fibers between the medial border of the scapula and the neural tissues in the back, which seemed to correspond to the *rhomboideus major* and *minor*. The left *triceps brachii*,

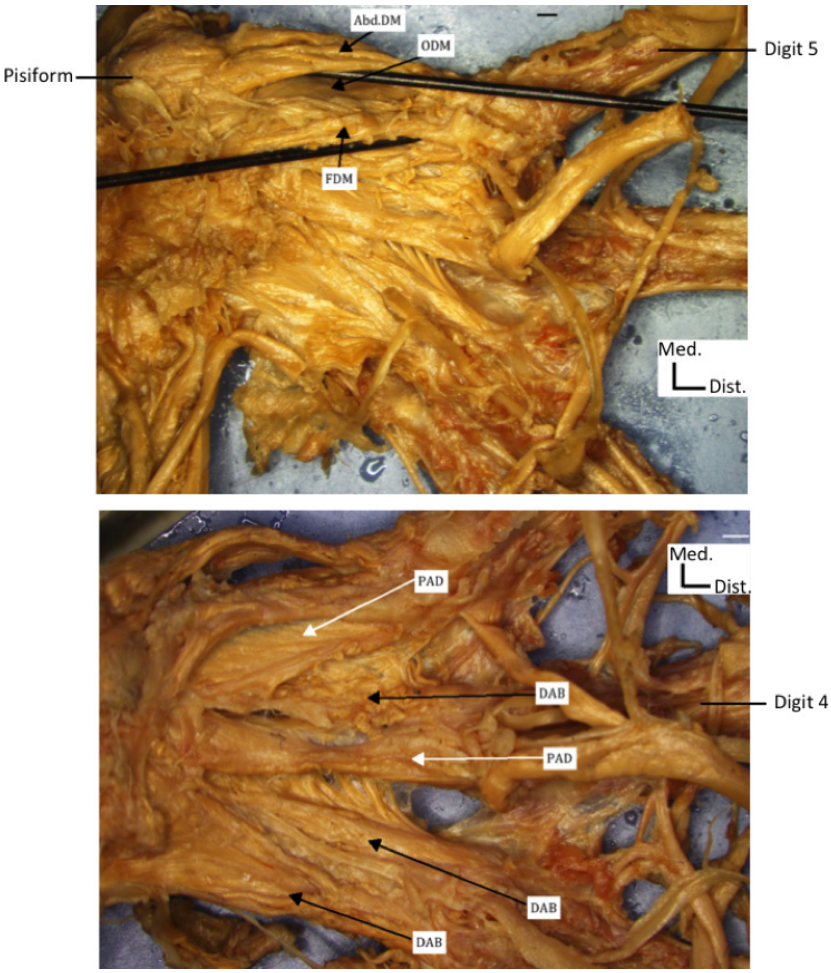

Fig. 11 Anterior view of the right hand of the fetus with craniorachischisis showing hypothenar muscles (upper figure) and dorsal (DAB) and palmar (PAD) interossei muscles (lower figure). Note that, contrary to the previous figures, the photographs, imaging, and labeling were done with software connected to microscope (see Material and Methods). AbdDM, abductor digiti minimi; ODM, opponens digiti minimi; FDM, flexor digiti minimi. Scale bar: 1 cm.

like the right one, had four heads. The extra head went from the lateral side of the humerus inferior to the deltoid and next to the *brachialis*. The insertion and innervation of the triceps was normal. The anterior arm muscles showed minimal abnormal morphology, the only major anomaly being that they were apparently innervated by the median nerve and not by the musculocutaneous nerve.

The *pronator teres*, *flexor carpi radialis*, *flexor carpi ulnaris*, and *flexor digitorum superficialis* had a normal origin but the flexor carpi radialis and flexor digitorum superficialis had abnormal insertions onto the trapezoid and digits 2, 3, and 4 only (to their middle phalanges, as usual). In addition, the proximal ends of pronator teres, flexor carpi ulnaris, and flexor digitorum superficialis were fused, and there was a separate head of the flexor carpi ulnaris from the olecranon process of the ulna. The *flexor digitorum profundus* had an almost normal configuration, with the exception that on its distal attachment at the 5th digit, a small tendon extended from the main tendon and attached to the middle phalanx of this digit (normally the muscle only goes to distal phalanges). Similarly, the *flexor pollicis longus* inserted onto the proximal ends of the distal (as usual) and proximal (an anomaly) phalanges of the thumb. A short, wide muscle slip was observed between the flexor pollicis longus and flexor digitorum profundus. The attachments of the *pronator quadratus* were as usual.

The *brachioradialis* had a normal origin, but it had two tendons: one attached to the distal end of the radius as usual, whereas the other attached to the base of metacarpal 1, being bifurcated and surrounding the tendon of the *abductor pollicis longus*, then distally forming again a single tendon. The long, superficial extensors had essentially normal attachments, with the exceptions that one of the tendons of the *extensor digitorum* split and attached onto both digits 4 and 5, and that the tendon of the *extensor digiti minimi* split at base of metacarpal 5 to attach to these two digits as well. Regarding the deeper extensors, the *abductor pollicis longus* arose from the posterior shaft of the radius and its tendon abnormally pierced the second tendon of the brachioradialis and attached to the palmar fascia. The *extensor pollicis brevis* also arose from the posterior shaft of the radius and its belly was abnormally fused with the abductor pollicis longus; abnormally, it also sent three tendons to a U-shaped connective tissue/fascia on the palmar lateral side of metacarpal 1. This U-shaped structure was also partially formed by the tendon of the *flexor*

pollicis longus. The *extensor pollicis longus* had a normal origin, but its distal tendon abnormally split at the base of metacarpal 1 and then formed again a single structure at the level of the metacarpophalangeal joint to attach to the dorsal side of the base of distal phalanx of the thumb, as usual. The *extensor indicis* originated from the posterior surface of the ulna and had a normal insertion. The *anconeus* and *supinator* essentially had normal attachments.

The muscles of the hand were also basically normal, with the following major exceptions. The *abductor pollicis brevis* attached distally to the abnormal U-shaped structure described in the paragraph above. The *opponens pollicis* had an abnormal attachment to the second tendon of the brachioradialis at the level of the base of metacarpal 1, and additionally inserted onto the proximal end of the distal phalanx of the thumb. The superficial head of the *flexor pollicis brevis* attached abnormally to the proximal end of the distal phalanx, whereas the deep head attached to the proximal phalanx as usual, but to its distal portion, which is a peculiar configuration.

Muscles of the right and left lower limbs (Tables S3 and S4)

The muscles of the right and the left lower limbs are grouped under a single section, unlike the muscles of the right and left upper limbs, because they were symmetrical, with a few exceptions due to the rare anomalies found in the lower limbs. Therefore, we will here only mention features that show anomalies; for more details about the attachments of all lower limb muscles, see Tables S3 and S4.

In the gluteal region, muscles of the right side were less differentiated and more difficult to separate than those on the left side. On the right side only, the *gluteus medius* was fused anteriorly with the *tensor fasciae latae*. The *extensor digitorum longus* had, on the right side of the body, an abnormal tendon slip extending from the tendon to digit 3 to the tendon to digit 4. In both sides of the body, the *flexor digitorum brevis* was missing its tendon to digit 5. On the right side, there was no *lumbricalis* to digit 2, and the transverse head of the *adductor hallucis* and the two heads of the *flexor hallucis brevis* were absent. On both sides of the body, the *extensor hallucis brevis* did not send a tendon to digit 4.

Muscles of the head (Tables S5 and S6)

The facial muscles were abnormally asymmetrical. On the right side, the muscles were less differentiated (fewer muscle fibers and more fat-like tissues) than those on the left side. Additionally, the muscles of mastication were less differentiated than the muscles of facial expression (Fig. 12). The *frontalis* muscles were located deep to a layer of fatty tissue, with normal fiber orientation and attachment. The *procerus* was represented by a thin layer of fibers between the eyes. The *orbicularis oculi* and *orbicularis oris* appeared normal on both sides. The *auricularis superior* and *posterior* were observed on the left side only: the superior was a thin band of muscle fibers running from the superior side of the ear to the superior side of the left eye, near the left frontalis; the posterior was a thin band of muscle fibers running between the postero-superior side of the ear to the posterior neural tissue. That is, both these muscles connected the ear to structures to which they never attach in normal individuals. In addition, the *auricularis anterior*, *corrugator supercilii*, *occipitalis*, *levator labii superioris alaeque nasi*,

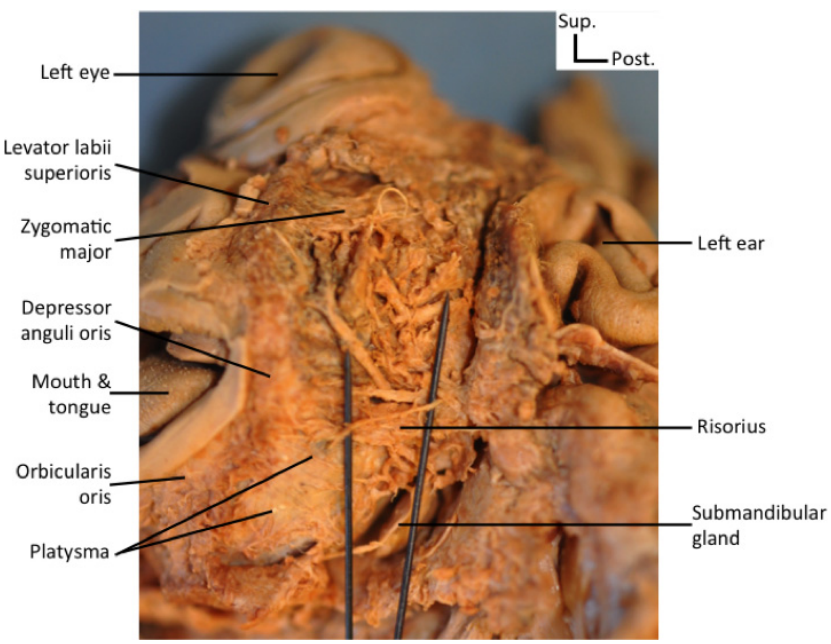

Fig. 12 Lateral view of the face of the left side of the body fetus with craniorachischisis, showing some facial muscles. Lt, left side.

levator anguli oris, and *depressor supercilii* were seemingly missing on both sides (Fig. 12).

Also on the left side only, the *levator labii superioris*, *zygomaticus major* and *minor*, and *risorius* were observed as antero-posteriorly directed muscle fibers (Fig. 12). The left *levator labii superioris* originated from the medial side of the eye region and inserted onto the corner of the upper lip. The *zygomaticus major* and *minor* originated from a region located inferior to the left eye and ear but inserted normally. The *risorius* was inferior to these three muscles, extending posteriorly from the posterior region of the mouth. None of previous muscles was observed on the right side. Muscle fibers could be observed on the left side of the head, between the nose, superiorly, and the mouth, inferiorly: these fibers might correspond to the *nasalis*. The *depressor anguli oris* extended bilaterally from the chin to the corners of the mouth, as usual. The *depressor labii inferior* was poorly differentiated on both sides of the head, being mainly connected to fat-like tissue, with few muscle fibers lying on the anterior/lateral surface of the chin region. The *mentalis* was located deep to the poorly differentiated depressor labii inferioris, being a thin layer of muscle fibers running mainly inferiorly towards the midline of the chin region. The *platysma* was a thin layer of multidirectional muscle fibers running from the latero-inferior borders of the mouth to posterior and inferior regions, on both sides (Fig. 12). Lastly, a strange muscle was observed over the nose that had oblique muscle fibers extended superiorly and laterally from the midline of the nose toward the eyes. The *buccinatorius* and *masseter* were mainly undifferentiated muscle structures lying antero-medial to the ears. Another undifferentiated muscle tissue was found between the lateral side of the left eye and the superior side of the left ear, seemingly corresponding to the left *temporalis*. Muscle fibers were also seen on the left side between the upper jaw (maxilla) and lower jaw (mandible), which may correspond to one *pterygoideus medialis*. The *pterygoideus lateralis* was therefore apparently missing on both sides, and the temporalis and medial pterygoid were seemingly missing on the right side.

The muscles of the neck were asymmetrical, with the ones on the right side being more abnormal and less differentiated than those of the left side (Fig. 13). The right *digastric* was fused with the mylohyoid, missing its characteristic

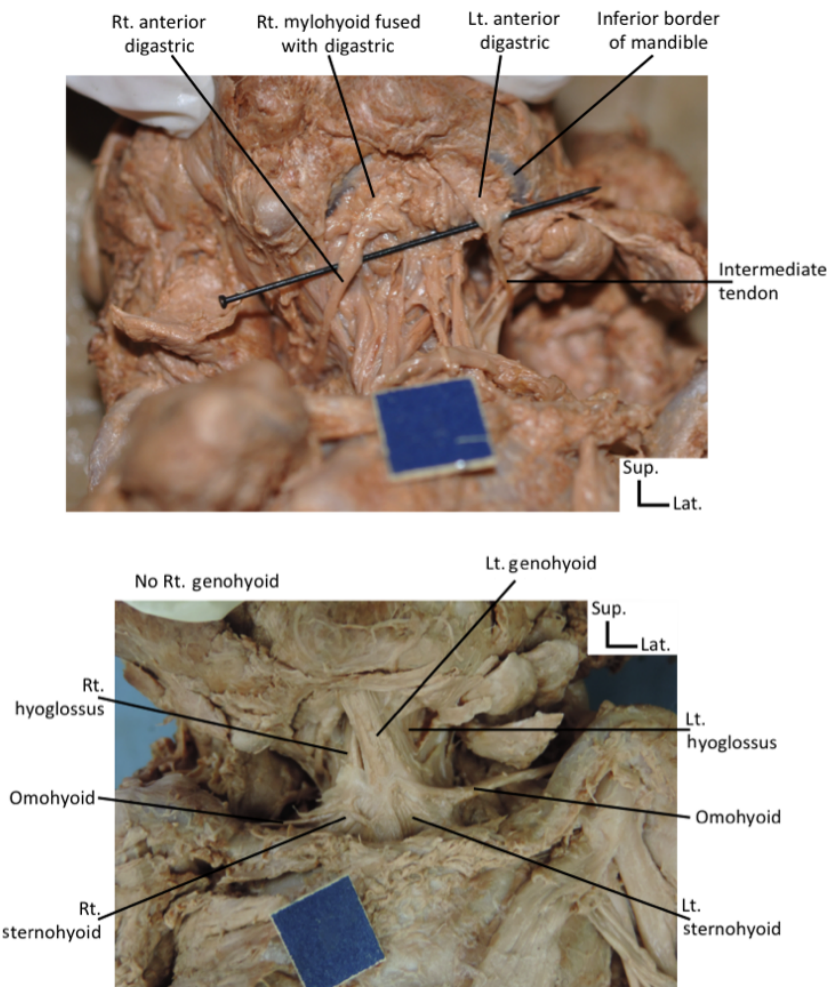

Fig. 13 Anterior views of the neck of the fetus with craniorachischisis, showing the muscles of the neck, including the intermediate tendon between the anterior and posterior digastric muscles. Note that the right geniohyoid muscle is apparently missing. Lt, left; rt, right. Scale bar: 1 cm.

intermediate tendon and fibrous loop – a feature probably related to the non-formation of a completely hyoid bone – and being posteriorly attached to the 'temporo-occipital' bone (Fig. 13). The anterior belly of the left *digastric* attached to the inferior border of the mandible, its attachment being wider than normal; there was an intermediate tendon but no fibrous loop, and the posterior belly attached posteriorly to 'temporo-occipital' bone (Fig. 13). There was a tendon slip extending antero-inferiorly from its intermediate tendon to fascia over the left *mylohyoideus*. The right mylohyoid was fused with the right digastric, being reduced in size and fused with the left mylohyoid, which was attached laterally to the inner side of the inferior border of the mandible and medially to fascia lying in the midline of the neck (Fig. 13).

The left *geniohyoideus* was a broad muscle extending from the hyoid region to the mandible as usual, but extending more lateral than normal, and being fused with the genioglossus; the right geniohyoid was absent (Fig. 13). The right *hyoglossus* extended from the hyoid region to the tongue as usual, but it was overall more medially located than normal. The left *hyoglossus* was deep and lateral to left geniohyoid and extended from the hyoid region to the tongue as usual but was fused with the styloglossus (Figs 13 and 14). On both sides, the *genioglossus* extended from the mandible to the tongue as usual, not being fused with the hyoglossus (Fig. 14). The right *styloglossus* originated from the prominent styloid process and 'temporo-occipital' bone and inserted onto the outer side of mandible, lateral to the hyoglossus; the left styloglossus was seemingly missing (Fig. 14).

Regarding the infrahyoid muscles, the *sternohyoideus* muscles originated from their normal positions at the sternum and extended to the hyoid region as usual, but they were fused with the proximal part of the omohyoid as well as to each other (Fig. 13). The right and left *omohyoideus* were strap-like muscles attached to the superior border of the scapula and to the hyoid region, as usual, but they had no intermediate tendon.

Regarding the branchial muscles, the *stylopharyngeus*, *tensor veli palatini* and *tensor tympani* were all seemingly absent, as were all pharyngeal muscles except the *palatoglossus* muscles, which connected the tongue to the soft palate, as usual. Despite the apparent absence of the pharyngeal constrictors, including the inferior ones, the *cricothyroideus* muscles (which are derived from the inferior pharyngeal muscles) were present and normal. In fact, the overall configuration of the laryngeal muscles was mainly normal, as is detailed in Table S6.

Lastly, the *trapezius* muscle – a branchial muscle that starts its development in the head region but then migrates to the back – was present on both sides, extending between the superior border of the scapular spine, the acromion process, the lateral third of the clavicle, and the supraoccipital

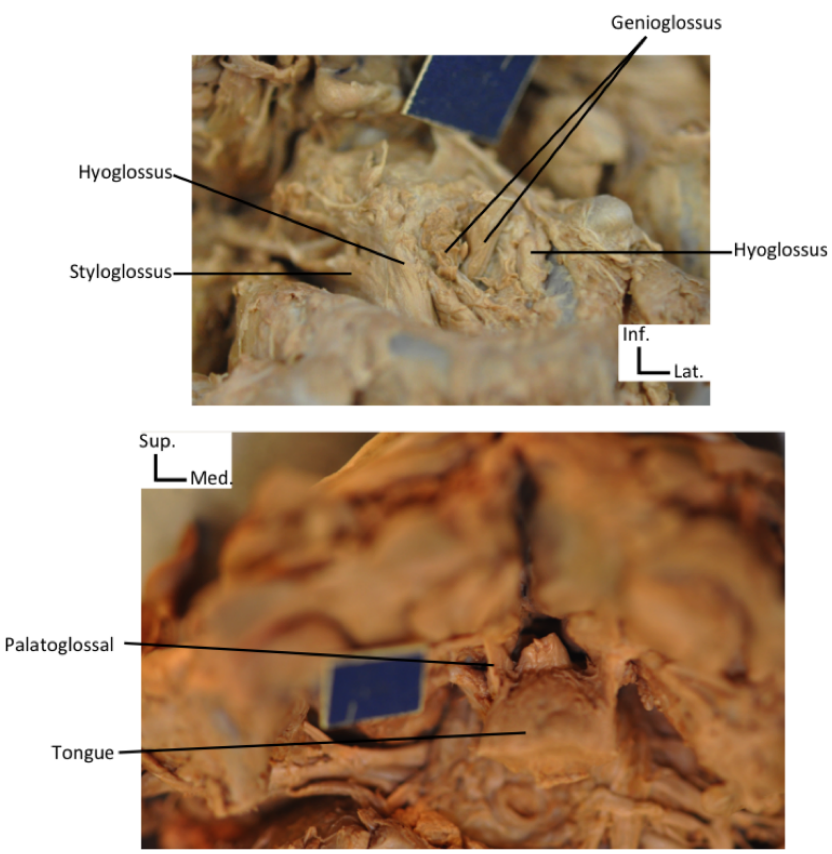

Fig. 14 Inferior (upper figure) and anterior (lower figure) views of the fetus with craniorachischisis, showing the tongue and associated muscles, which include the pharyngeal palatoglossal muscle. Scale bar: 1 cm.

bone. The right trapezius was less differentiated, being located between the right eye and shoulder. The tissues were attached to the spine of the scapula inferiorly, to the supraoccipital bone postero-laterally, and to the right *sternocleidomastoideus* muscle internally.

Discussion

The open cranium and open vertebral column without a brain and spinal cord indicate a severe developmental defect during neurulation. Normally, during early neurulation the paraxial mesoderm forms whorl-like structures called somitomeres parasagittal to the notochord. Most somitomeres form somites, but the somitomeres in the head region never form somites. The neural crest cells originate from cells at the border of ectoderm and neuroectoderm and start migrating between the ectoderm and mesoderm before the neural tube closes.

Cranial neural crest cells (NCCs) migrate with mesodermal cells into the developing pharyngeal arches and give rise to most skeletal elements of the head (Le Douarin et al. 1993). The thyroid, arytenoid, and cricoid cartilages appeared normal in our fetus, but all rostral cranial structures were malformed. This indicates that the neural crest derivatives of the pharyngeal arches 4 and 6 are less affected than the anterior pharyngeal arches 1–3, which form the viscerocranium (1st arch: maxilla, zygomatic bone, squamous portion of temporal bone; 2nd arch: styloid process) and the hyoid bone (2nd and 3rd arch derivative). NCCs start migrating before the closure of the neural tube but in a rostro-caudal wave, indicating that the most rostral neural crest streams were the most severely affected by the disruption of the neurulation in the described fetus. This is in line with the observation that the malformations in the cranium are the most severe, followed by the shoulder girdle and the upper limb, whereas the pelvic girdle and the lower limbs appear to be more normal.

Cranial NCCs surround muscle anlagen, influencing the muscle and connective tissue patterning (Noden, 1983; Ericsson et al. 2009). Still, cranial muscles, except extraocular muscles, form in the absence of cranial NCCs (Noden & Trainor, 2005). Therefore, the role of those cells during cranial muscle development is likely due to the cranial NCC-derived connective tissue that gradually imposes the typical anatomical musculoskeletal design on pharyngeal mesoderm muscle precursors (Rinon et al. 2007). As observed for the skeletal features in our fetus, the muscle abnormalities decrease from the rostral to caudal. The overall configuration of the laryngeal muscles was mainly normal, indicating again that the derivatives of the 4th and 6th pharyngeal arches are less affected than the first three arches.

Furthermore, skeletal and muscular malformations were more severe on the right side of the fetus than on the left side. Therefore, we hypothesize that the neural crest migration was more disturbed on the right side than on the left side of the fetus, which would explain the observed asymmetric abnormalities in both skeletal and muscular tissues.

The skeletal components of the upper and lower limbs form from the lateral plate mesoderm, and the muscular components form from the dorsal part of the somites, i.e. the dermomyotome. During dermomyotome development, signals from the neural tube, and adjacent tissues cause a medio-lateral patterning (Christ & Brand-Saberi, 2004). Malformations commonly increase from proximal to distal (Smith et al. 2015), as was also described in the upper limbs of our fetus. The proximal elements (pectoral and pelvic girdles, humerus/femur, radius & ulnar/fibula & tibia) were normal, whereas the distal elements in the right wrist and hand were abnormal (reduced), but the distal elements of the lower limb were mainly normal, on both sides of the body. The patterning of the distal parts of the limbs is dependent upon specific gene signaling. As the pectoral and pelvic girdles were essentially normal, we hypothesize that the development of somites was not highly disturbed *per se*: instead, it is the later differential patterning of the distal extremities that might have been affected by defects that also caused the defects during neurulation.

There are almost no descriptions of the musculoskeletal system in humans with neural tube defects, in particular those with anencephaly. One of the very few exceptions is Windle (1893), who described muscle anomalies in 10 anencephalic fetuses, five females and five males. It is therefore worth summarizing the anomalies reported by him, in order to compare them with the results obtained in the fetus analyzed by us. Of the 25 anomalies described by him, five were similar to configurations found in the fetus dissected by us. He described the presence of an additional portion of the pectoralis major, which arose from the false ribs and from the aponeurosis of the external oblique muscle and inserted onto the humerus on the left side in one female and both sides in one male. We also found an additional bundle of the pectoralis major on the left upper limb of the fetus examined by us. Windle also reported the presence of an axillary sling from the latissimus dorsi to two tendons inserting onto the pectoralis major on the right side in one female. On the right side of the fetus we analyzed, a connection between the pectoralis major and latissimus dorsi, via the abnormal dorsoepitrochlearis muscle was present. Windle also described the absence of the palmaris longus on the right side in one male, on the left side in another male, and on both sides of one male; this muscle was missing on the left side of the fetus dissected by us. However, it should be noted that in 'normal' humans the absence of the palmaris longus is a comment variation. Windle furthermore reported a flexor digitorum superficialis with no tendon to digit 5 on the right side in one male, and the presence of two special extensors to the little finger, and one extensor digiti medii (i.e. a distinct, deep extensor going exclusively to digit 3), as well as the normal tendons from the extensor digitorum on the right side in one

female. On the left side of the fetus dissected by us, the flexor digitorum superficialis also lacked a tendon to digit 5, and the long extensor tendons that normally attach to a single digit were subdivided into tendons going to more than one digit.

The other 20 anomalies described by Windle (1893) were: (1) the muscle platysma was unusually well developed and extended for some distance over the surface of the thorax in one female; (2) the anterior belly of the omohyoid was represented by a band of fibrous tissue destitute of muscular fibers on the left side of one female; (3) presence of a sternalis muscle (supernumerary muscle) on the left side in two females and one male, and on the both sides in one female; (4) presence of a muscular slip arising by a tendon from the outer side of the short head of the biceps brachii and inserting onto the humerus near the insertion of the coracobrachialis on both sides in one male; (5) presence of fleshy fibers of the triceps that are continuous with those of the anconeus on the right side in two males; (6) presence of a muscular slip from the brachioradialis to the supinator on the right side in one male; (7) extensor carpi radialis longus inserting by two distinct tendons on the right side in one male; (8) presence of double palmaris longus on the left side in one female; (9) presence of a small muscular slip from the inner condyle of the humerus to the outermost part of the flexor digitorum profundus on the left side in one female and both sides of one female; (10) presence of extensor digiti medii on the right side in one male; (11) presence of two special extensors of the index finger, besides the slip from the extensor digitorum, on the right side in one female; (12) presence of a second extensor pollicis longus, arising together with the extensor indicis, on the left side in one male; (13) presence of a detached muscle lying in front of the psoas major, occupying the position of the psoas minor and inserting onto the lesser trochanter of the femur on both sides in one female; (14) psoas major divided into two portions, one being external to the other and smaller and inserting together, on the right side in one male; (15) absence of a straight head of the rectus femoris on the left side in one female; (16) extensor hallucis longus of the left side supplied an 'extensor primi internodii hallucis' accessory tendinous slip that inserted onto the proximal phalanx of the big toe, in one female; (17) extensor hallucis longus inserted by two tendons on one side in one male; (18) absence of the plantaris on the right side in one male and one female; (19) presence of a condylar head of the flexor hallucis longus on the right side in one male and on the left side in one male; and (20) the fibularis tertius formed the greater part of the muscular belly of the extensor digitorum longus on the left side in one female, and had an unusually large muscular portion in one male.

Moreover, Wheeler (1918) described some muscular anomalies in the trunk of a fetus with spina bifida with encephaloceles that somewhat resembled what was seen in the present study. One anomaly he reported is that the trapezius was represented by strap-like bands of muscle originating from fascia over the cervical and thoracic vertebrae. Another one was that the rhomboidei were very thin and short muscles. In the fetus we analyzed, the trapezius and rhomboids were thin structures, very reduced in volume or seemingly completely absent. Other anomalies reported by Wheeler (1918) were: (1) despite normal origins, insertions, and sizes of the levator scapulae muscles, the muscle fibers were directed horizontally instead of slanting downwards as usual; (2) unidentifiable serratus posterior muscles; and asymmetrical serratus anterior muscles.

Regarding the skeleton system, defects found in the fetus analyzed by us, such as radial deficiency, also resembled defects that were reported in many other cases associated with a wide range of other syndromes (Secord, 1915; Kato, 1924; Harbeson, 1937). Additional examples are the bowing of the ulna, the absence of the thumb and of the thenar musculature (Manske et al. 1995), and the reduction/loss of digit 2 (Buckwalter et al. 1981; Miura, 1988; Rayan & Upton, 2014). Similarly, absence of some parts of the cranial vault as seen in the examined fetus could be due to the absence of the brain, as reported for other pathological cases, as formation of the brain is necessary for initiation of ossification of the dermal skull roof (Carlson, 1981). Conditions such as cleft lip and palate are also found in a wide range of syndromes, and are possibly related to developmental delay or arrest, which result in a failure of fusion between the maxillary and frontonasal protuberances (Dudas et al. 2007).

Furthermore, several anomalies found in the anencephalic fetus examined by us are also seen in fetuses with conditions that might be partially related mechanistically, such as trisomies 13, 18, and 21 – as neural tube defects have been associated with such chromosomal defects (Wyszynski, 2006; Lazareff, 2011) – but that anatomically are strikingly different from the configuration of this fetus, such as cyclopia. A detailed list of common muscular anomalies found in a wide range of pathological conditions and syndromes was recently given by Smith et al. (2015) and discussed by Diogo et al. (2015). We will, therefore, list here those that are also found in the fetus examined in the present study: (1) presence of occipital rhomboid; (2) marked asymmetry between muscles of left and right sides of the body; (3) abnormal 'costohumeralis' bundle of pectoralis major; (4) abnormal dorsoepitrochlearis muscle; (5) abnormal fusions, e.g. coracobrachialis and dorsoepitrochlearis/pectoralis major; (6) digitorum superficialis lacking a tendon to digit 5; (7) slips between pectoralis major and minor; (8) slips between flexor pollicis longus and flexor digitorum profundus; (9) absence of palmaris longus; (10) presence of more tendons of the forearm extensors to digits; (11) flexor digitorum brevis missing the tendon to digit 5 of the foot; and (12) fusion between mylohyoid and digastric.

As recently pointed out by Diogo et al. (2015), the fact that similar anomalies are seen commonly not only in a

wide range of different syndromes, but also as variants of the normal human population and as the 'normal' phenotype of other animals, supports Pere Alberch's (1989) unfortunately named 'logic of monsters'. That is, it supports the view that development is so constrained that both in 'normal' and abnormal development one sees certain outcomes being produced again and again because ontogenetic constraints only allow a few possible outcomes, thus also leading to cases where the anatomical defects of some organisms are similar to the 'normal' phenotype of other organisms. The examination of the fetus studied by us further reinforces this view, because some of the defects can for instance be due to developmental delay/arrest, a pattern seen frequently in cases of human congenital malformations (Diogo & Wood, 2012, 2013, 2016; Diogo et al. 2015; Smith et al. 2015). These include, for instance: the fusion between/slips connecting the coracobrachialis and pectoralis major, which develop from the ventral limb primordium; the slip between the pectoralis major and minor, which develops from the pectoralis primordium; the slips between the flexor pollicis longus and the flexor digitorum profundus, as the former muscle derives evolutionary and developmentally from the latter; fusion between the mylohyoid and the anterior part of the digastric, as both these structures derive from the first arch primordium. In fact, it is remarkable that all these features that are abnormally seen in this fetus, when compared with a 'normal' fetus of the same age, are among the features that normally are found within a wide range of syndromes and pathological conditions, such as those listed above.

Another point supporting Alberch's idea that there is a 'logic', or predictable 'order', even in cases of extreme congenital malformations, is that in all those syndromes/conditions which affect several areas of the body, one sees the same pattern concerning the distribution of the muscle anomalies, e.g. the upper limbs being more defective than the lower (Diogo et al. 2015). That is, in such extreme congenital malformations affecting all regions of the body, one could expect to see a chaotic, random distribution of defects within the different body parts among different syndromes/conditions, for instance due to a general lack of homeostasis (e.g., Shapiro et al. 1983). However, this is not what we found. Instead, the same general patterns, as well as the same specific anatomical anomalies, recur in these different syndromes and conditions, as predicted by Pere Alberch. Such general patterns are, again, seen in the fetus examined for this study: it had 29 muscle anomalies on the right upper limb and 22 muscle anomalies on the left upper limb, vs. seven muscle anomalies on the right lower limb and two on the left lower limb. Another general pattern seen in different syndromes/conditions is the occurrence of a high left–right asymmetry: in this specific case, the total number of anomalies specifically found in the right upper and lower limbs (36) is remarkably higher than that seen in the left upper and lower limbs (24).

The present study not only provides the first detailed report of the musculoskeletal system of a fetus with craniorachischisis, which represents a substantial contribution to the medial and pathological literature, but also paves the way for broader discussions within the fields of comparative anatomy, evolution and developmental evolution, and evolutionary developmental biology. In particular, we hope to stimulate the undertaking of further studies on the musculoskeletal system of human individuals with other pathological conditions/syndromes, and broader comparisons of anomalies related with them, as well as of variations found in the 'normal' human population.

Acknowledgements

We are particularly thankful to the family who donated the fetus for scientific investigation. Furthermore, we are grateful to Marjorie Gondre-Lewis, Julia Molnar, and Christopher Smith for helpful discussions and suggestions. We acknowledge the College of Medicine at Howard University for the start-up funds assigned to Rui Diogo, as well as the King Saud University for Health Sciences and Saudi Arabian Cultural Mission for Malak Alghamdi's PhD grant.

References

Alberch P (1989) The logic of monsters: evidence for internal constraint in development and evolution. *Geobios* **22**, 21–57.

Bardeen CR, Lewis WH (1901) Development of the limbs, body-wall and back in man. *Am J Anat* **1**, 1–35.

Buckwalter JA, Flatt AE, Shurr DG, et al. (1981) The absent fifth metacarpal. *J Hand Surg* **6**, 364–367.

Carlson BM (1981) Summary. In: *Morphogenesis and Pattern Formation* (eds Connelly TG, Brinkley LL, Carlson BM), pp. 289–293. New York: Raven Press.

Christ B, Brand-Saberi B (2004) Limb muscle development. *Int J Dev Biol* **46**, 905–914.

Colas JF, Schoenwolf GC (2001) Towards a cellular and molecular understanding of neurulation. *Dev Dyn* **221**, 117–145.

Coskun A, Kiran G, Ozdemir O (2009) Craniorachischisis totalis: a case report and review of the literature. *Fetal Diagn Ther* **25**, 21–25.

Detrait ER, George TM, Etchevers HC, et al. (2005) Human neural tube defects: developmental biology, epidemiology, and genetics. *Neurotoxicol Teratol* **27**, 515–524.

Diogo R, Wood B (2011) Soft-tissue anatomy of the primates: phylogenetic analyses based on the muscles of the head, neck, pectoral region and upper limb, with notes on the evolution of these muscles. *J Anat* **219**, 273–359.

Diogo R, Wood B (2012) *Comparative Anatomy and Phylogeny of Primate Muscles and Human Evolution*. Oxford: Taylor and Francis.

Diogo R, Wood B (2013) The broader evolutionary lessons to be learned from a comparative and phylogenetic analysis of primate muscle morphology. *Biol Rev* **88**, 988–1001.

Diogo R, Wood B (2016) Origin, development, and evolution of primate muscles, with notes on human anatomical variations and anomalies. In: Boughner J, Rolian C (eds.), *Developmental approaches to human evolution*, Hoboken: John Wiley & Sons: 167–204.

Diogo R, Smith C, Ziermann JM (2015) Evolutionary developmental pathology and anthropology: a new area linking development, comparative anatomy, human evolution, morphological variations and defects, and medicine. *Dev Dyn* **244**, 1357–1374.

Dudas M, Li WY, Kim J, Yang A, Kaartinen V (2007) Palatal fusion - where do the midline cells go? A review on cleft palate, a major human birth defect. *Acta Histochem* **109**, 1–14.

England MA (1983) *Color atlas of life before birth – normal fetal development*. Chicago: Year Book.

Ericsson R, Ziermann JM, Piekarski N, et al. (2009) Cell fate and timing in the evolution of neural crest and mesoderm development in the head region of amphibians and lungfishes. *Acta Zool (Stockholm)* **90**, 264–272.

Golden JA, Chernoff GF (1995) Multiple sites of anterior neural tube closure in humans: evidence from anterior neural tube defects (anencephaly). *Pediatrics* **95**, 506–510.

Harbeson AE (1937) Bilateral congenital absence of the radii. *Can Med Assoc J* **36**, 359–360.

Kato K (1924) Congenital absence of the radius. *J Bone Joint Surg* **6**, 589–626.

Keiller VH (1922) A contribution to the anatomy of spina bifida. *Brain* **45**, 31–103.

Klein A (2013) *Neural Tube Defects: Prevalence, Pathogenesis and Prevention*. New York: Nova Science Publishers.

Lazareff JA (2011) *Neural Tube Defects*. Singapure: World Scientific.

Le Douarin NM, Ziller C, Couly GF (1993) Patterning of neural crest derivatives in the avian embryo: in vivo and in vitro studies. *Dev Biol* **159**, 24–49.

Lewis WH (1902) The development of the arm in man. *Am J Anat* **1**, 145–183.

Lewis WH (1910) The development of the muscular system. In: *Manual of Human Embryology*, vol. **1** (eds. Keibel F, Mall FP), pp. 454–522. Philadelphia: Lippincott.

Manske PR, McCarroll HR, James M (1995) Type III – a hypoplastic thumb. *J Hand Surg* **20**, 246–253.

Miura T (1988) Congenital absence of the fourth metacarpal bone (congenital dysplasia of the ring finger). *J Hand Surg* **13**, 93–96.

Moore CM, Dick EJ, Hubbard GB, et al. (2011) Craniorachischisis and omphalocele in a stillborn cynomolgus monkey (*Macaca fascicularis*). *Am J Med Genet A* **155**, 1367–1373.

Nañagas JC (1925) A comparison of the growth of the body dimensions of anencephalic human fetuses with normal fetal growth as determined by graphic analysis and empirical formulae. *Am J Anat* **35**, 455–494.

Netter FH (2012) *Frank H. Netter's Atlas of Human Embryology*. Philadelphia: Elsevier/Saunders.

Noden DM (1983) The role of the neural crest in patterning of avian cranial skeletal, connective, and muscle tissues. *Dev Biol* **96**, 144–165.

Noden DM, Trainor PA (2005) Relations and interactions between cranial mesoderm and neural crest populations. *J Anat* **207**, 575–601.

Oostra RJ, Baljet B, Hennekam R (1998) Congenital anomalies in the teratological collection of Museum Vrolik in Amsterdam, The Netherlands. IV: Closure defects of the neural tube. *Am J Med Genet* **80**, 60–73.

Rao TR, Shetty P, Rao S (2009) Additional slip of pectoralis major muscle: the costohumeralis. *Int J Anat Var* **2**, 35–37.

Rayan GM, Upton J (2014) *Congenital Hand Differences and Associated Syndromes*. Berlin: Springer.

Rinon A, Lazar S, Marshall H, et al. (2007) Cranial neural crest cells regulate head muscle patterning and differentiation during vertebrate embryogenesis. *Development* **134**, 3065–3075.

Schoenwolf GC, Bleyl SB, Brauer PR, et al. (2015) *Larsen's Human Embryology*. 5th edn. Philadelphia: Elsevier Saunders.

Secord ER (1915) Bilateral congenital absence of the radius. *Ann Surg* **61**, 380–381.

Shapiro BL, Hermann J, Opitz JM (1983) Down syndrome – a disruption of homeostasis. *Am J Med Genet* **14**, 241–269.

Smith CM, Ziermann JM, Molnar J, et al. (2015) *Muscular and Skeletal Anomalies in Human Trisomy in an Evo-Devo Context: Description of a T18 Cyclopic Fetus and Comparison Between Edwards (T18), Patau (T13) and Down (T21) Syndromes Using 3-D Imaging and Anatomical Illustrations*. Boca Raton: CRC Press.

Sucheston ME, Cannon MS (1970) Microscopic comparison of the normal and anencephalic human adrenal gland with emphasis on the transient-zone. *Obstet Gynecol* **35**, 544–553.

Van Allen MI, Kalousek DK, Chernoff GF, et al. (1993) Evidence for multi-site closure of the neural tube in humans. *Am J Med Genet* **47**, 723–743.

Vare AM, Bansal PC (1971) An anatomical study of 41 anencephalics. *Indian J Pediatr* **38**, 301–305.

Wheeler T (1918) *Study of a Human Spina Bifida Monster with Encephaloceles and Other Abnormalities*. Washington, DC: Carnegie Institution of Washington.

Windle BC (1893) The myology of the anencephalous foetus. *J Anat Physiol* **27**, 348–353.

Wyszynski DF (2006) *Neural Tube Defects: From Origin to Treatment*. Oxford: Oxford University Press.

Supporting Information

Additional Supporting Information may be found in the online version of this article:

Table S1 Right upper limb muscles.
Table S2 Left upper limb muscles.
Table S3 Right lower limb muscles.
Table S4 Left lower limb muscles.
Table S5 Facial muscles and masticatory muscles.
Table S6 Muscles of the neck.